Cancer Cell
Article

The JAK2 Inhibitor AZD1480 Potently Blocks Stat3 Signaling and Oncogenesis in Solid Tumors

Michael Hedvat,[1] Dennis Huszar,[3] Andreas Herrmann,[2] Joseph M. Gozgit,[3] Anne Schroeder,[1] Adam Sheehy,[3] Ralf Buettner,[1] David Proia,[3] Claudia M. Kowolik,[1] Hong Xin,[2] Brian Armstrong,[1] Geraldine Bebernitz,[3] Shaobu Weng,[3] Lin Wang,[3] Minwei Ye,[3] Kristen McEachern,[3] Huawei Chen,[3] Deborah Morosini,[3] Kirsten Bell,[3] Marat Alimzhanov,[3] Stephanos Ioannidis,[3] Patricia McCoon,[3] Zhu A. Cao,[3] Hua Yu,[2] Richard Jove,[1,*] and Michael Zinda[3,*]
[1]Molecular Medicine
[2]Cancer Immunotherapeutics and Tumor Immunology
Beckman Research Institute, Irell & Manella Graduate School of Biological Sciences, City of Hope Cancer Center, Duarte, CA 91010, USA
[3]Cancer Bioscience, AstraZeneca R&D Boston, Waltham, MA 02451, USA
*Correspondence: rjove@coh.org (R.J.), michael.zinda@astrazeneca.com (M.Z.)
DOI 10.1016/j.ccr.2009.10.015

SUMMARY

Persistent activation of Stat3 is oncogenic and is prevalent in a wide variety of human cancers. Chronic cytokine stimulation is associated with Stat3 activation in some tumors, implicating cytokine receptor-associated Jak family kinases. Using Jak2 inhibitors, we demonstrate a central role of Jaks in modulating basal and cytokine-induced Stat3 activation in human solid tumor cell lines. Inhibition of Jak2 activity is associated with abrogation of Stat3 nuclear translocation and tumorigenesis. The Jak2 inhibitor AZD1480 suppresses the growth of human solid tumor xenografts harboring persistent Stat3 activity. We demonstrate the essential role of Stat3 downstream of Jaks by inhibition of tumor growth using short hairpin RNA targeting Stat3. Our data support a key role of Jak kinase activity in Stat3-dependent tumorigenesis.

INTRODUCTION

The signal transducer and activator of transcription (Stat) proteins comprise a family of transcription factors that mediate cytokine and growth factor responses (Akira et al., 1994; Darnell, 1997; Darnell et al., 1994). Persistent activation of Stat3 is oncogenic (Yu and Jove, 2004) and is prevalent in a wide variety of human cancers, including breast, prostate, head and neck, and ovarian cancers, among other solid and hematologic tumors (Bromberg et al., 1999; Catlett-Falcone et al., 1999; Dhir et al., 2002; Garcia et al., 2001; Grandis et al., 2000; Levy and Inghirami, 2006; Silver et al., 2004; Yu et al., 2007). Aberrant Stat3 activation is required for the survival of some types of human cancer cells by promoting the overexpression of genes that encode antiapoptotic proteins, cell-cycle regulators, and angiogenic factors (Bowman et al., 2000, 2001; Grandis et al., 2000; Niu et al., 2002b).

Stat3 is activated by phosphorylation of Tyr705, promoting cytosolic dimerization, nuclear translocation, and DNA binding (Darnell et al., 1994). Stat activation by cytokines is mediated through the Janus family kinases (Jak), which include four family members, Jak1, Jak2, Jak3, and Tyk2 (Schindler and Darnell, 1995). Jak1, Jak2, and Tyk2 are ubiquitously expressed, whereas expression of Jak3 is primarily restricted to the lymphoid lineage (Johnston et al., 1994). Jak family kinases associate with the large hematopoietin subfamily of cytokine receptors that lack intrinsic kinase activity and are dependent on Jak catalytic activity for signal transduction (Leaman et al., 1996). In addition, Stat3 can be phosphorylated by activated growth factor receptors such as c-MET and EGFR (Boccaccio et al., 1998; Quesnelle et al., 2007). Src family kinases have also been implicated in Stat3 activation (Bowman et al., 2000).

A growing body of evidence has documented an important role for autocrine and/or paracrine cytokine loops in driving aberrant activation of Stat3 in human cancer. In particular, interleukin-6 (IL-6) signaling has been implicated in tumorigenesis (Catlett-Falcone et al., 1999; Grivennikov et al., 2009; Hodge et al., 2005; Hong et al., 2007). Recent studies in breast (Berishaj

SIGNIFICANCE

Development of small molecule inhibitors of Jak2 for the treatment of myeloproliferative neoplasms provides an opportunity to assess the role of persistent Jak/Stat activation in solid tumors. Chronic cytokine stimulation is associated with constitutive Stat3 activation in many types of tumors, contributing to growth and survival. Using the Jak2 inhibitor AZD1480, we demonstrate the central role of Jak family kinases in Stat3 activation and growth of human solid tumor xenografts. Our data provide support for the further development of Jak2 inhibitors for treatment of solid tumors.

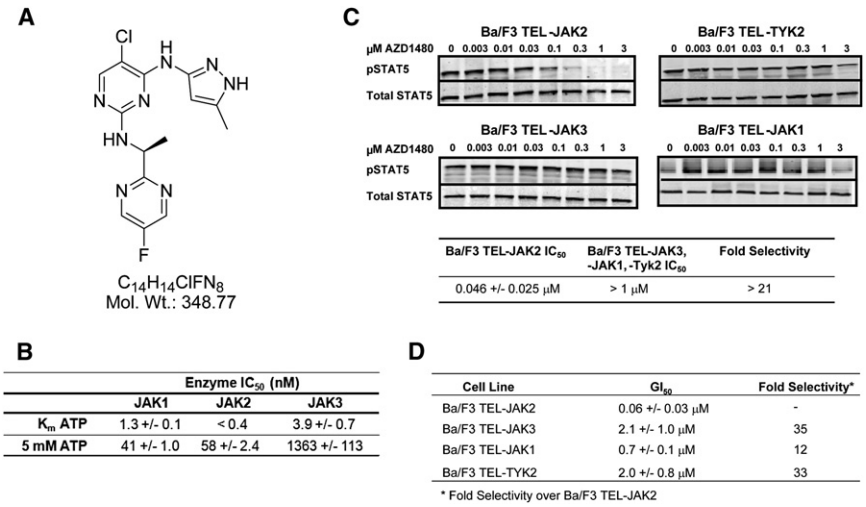

Figure 1. Janus Kinase Family Selectivity of AZD1480

Jak family kinase selectivity was determined using both enzymatic assays and Ba/F3 cells engineered to express constitutively active Jak kinases by fusing the kinase domain of Jak1, Jak2, Jak3, and Tyk2 with the dimerization domain of TEL.

(A) Chemical structure of AZD1480.

(B) Jak1, Jak2, and Jak3 enzymatic assays were carried out in triplicate at K_m levels of ATP and 5 mM ATP. Ranges depicted represent ± SD.

(C) Inhibition of Stat5 phosphorylation in Ba/F3 TEL-Jak2, TEL-Jak3, TEL-Jak1, and TEL-Tyk2 cells. TEL-Jak cells were treated with the indicated concentrations of AZD1480 for 1 hr and the levels of phospho-Stat5 were determined by western immunoblotting. Signal intensity was quantified using Li-Cor Odyssey software. IC_{50} values were calculated from a minimum of three independent experiments. Ranges depicted represent ± SD.

(D) Inhibition of Jak1, Jak2, Jak3, and Tyk2 kinase-driven cellular proliferation in engineered Ba/F3 cell lines. TEL-Jak cells were plated in 96-well plates, treated 24 hr later with AZD1480, and incubated for 48 hr. Cell proliferation was determined using the Alamar blue assay. GI_{50} values were calculated from a minimum of four independent experiments. Ranges depicted represent ± SD.

et al., 2007), lung (Gao et al., 2007), and diffuse large B cell lymphoma (Lam et al., 2008) cancer cell lines have demonstrated a central role of Jak family kinases in mediating IL-6 signaling in these cells. These observations provide a molecular basis for constitutive Stat3 activation in solid tumor types and highlights Jaks as potential targets for cancer therapy.

The recent identification of an acquired Jak2 mutation in myeloproliferative neoplasms has led to the rapid development of selective Jak2 small-molecule inhibitors (Levine and Gilliland, 2008; Morgan and Gilliland, 2008). These reagents provide a means of testing the involvement of Jaks in Stat3-dependent tumorigenesis. We have used the Jak2 inhibitors AZ960 (Gozgit et al., 2008) and AZD1480 to determine whether Jak2 is a central mediator of constitutive and inducible Stat3 activation in tumor cells and if inhibition of this signaling axis could suppress the growth of solid tumor xenografts.

RESULTS

In Vitro Characterization of AZD1480

The pyrazolyl pyrimidine AZD1480 is a potent ATP competitive inhibitor of Jak2 kinase, with an inhibition constant (Ki) of 0.26 nM (Figure 1A and Figure S1 available online). To evaluate Jak family selectivity of AZD1480, we carried out Jak1, Jak2, and Jak3 enzymatic assays at K_m levels of ATP and 5 mM ATP, the high end of ATP concentrations in cells (Figure 1B). AZD1480 demonstrated significant Jak2 selectivity over Jak3, in particular at high ATP concentrations and marginal selectivity over Jak1 at K_m ATP.

To evaluate the cellular selectivity of AZD1480 between the Jak family of kinases, we tested a panel of isogenic Ba/F3 cell lines driven by the JH1 catalytic domains of Jak1, Jak2, Jak3, or Tyk2 fused to the oligomerization domain of TEL (Gozgit et al., 2008; Lacronique et al., 2000). AZD1480 inhibited the phosphorylation of Stat5 with an IC_{50} of 46 nM in TEL-Jak2 cells, whereas little or no inhibition of Stat5 phosphorylation was observed in the TEL-Jak3, TEL-Jak1, or TEL-Tyk2 cells at or below 1 μM AZD1480 (Figure 1C). In these same cells, AZD1480 potently inhibited the growth of the TEL-Jak2 cell line with a GI_{50} of 60 nM. Proliferation of Ba/F3 cell lines bearing the other Jak family members was inhibited at much higher GI_{50} values in line with the selectivity observed in enzyme and/or pStat5 assays (Figure 1D).

To assess the overall kinase selectivity, we evaluated AZD1480 against a panel of 82 kinases (Millipore Corporation) at or near K_m for ATP with three drug concentrations (0.01, 0.10, and 1.0 μM). The kinases represent the diversity of the kinome based on kinase binding site similarity and the gatekeeper residue, a major determinant of small molecule kinase selectivity. Eleven out of 82 kinases, including Jak2, were inhibited by greater than 50% at 0.10 μM (Figure S2).

Jaks Are Central Mediators of Stat3 Signaling in Solid Tumor Cells

Screening of a panel of cell lines manifesting constitutive or inducible Stat3 tyrosyl phosphorylation demonstrated that in virtually all (17/18) of the lines $pStat3^{Tyr705}$ was dependent on Jak kinase activity (Figures 2A and 2B). Stat3 is activated downstream of Src family kinases and activated growth factor receptors, therefore the impact of Src, EGFR, and Met kinase inhibitors was also tested. Notably, neither inhibition of Src (15 cell lines tested) nor EGFR (seven cell lines tested) resulted in modulation of $pStat3^{Tyr705}$ in this panel of cell lines, despite complete inhibition of pSrc and pEGFR (Figure S3). Only c-Met inhibition in the gastric cell line MKN45 showed Jak2-independent inhibition of $pStat3^{Tyr705}$. These data indicate a central role of Jak family kinases in mediating Stat3 activation in solid tumor cell lines.

To further investigate the role of Jak kinases in modulating Stat3 activity, we used a murine embryonic fibroblast (MEF) cell

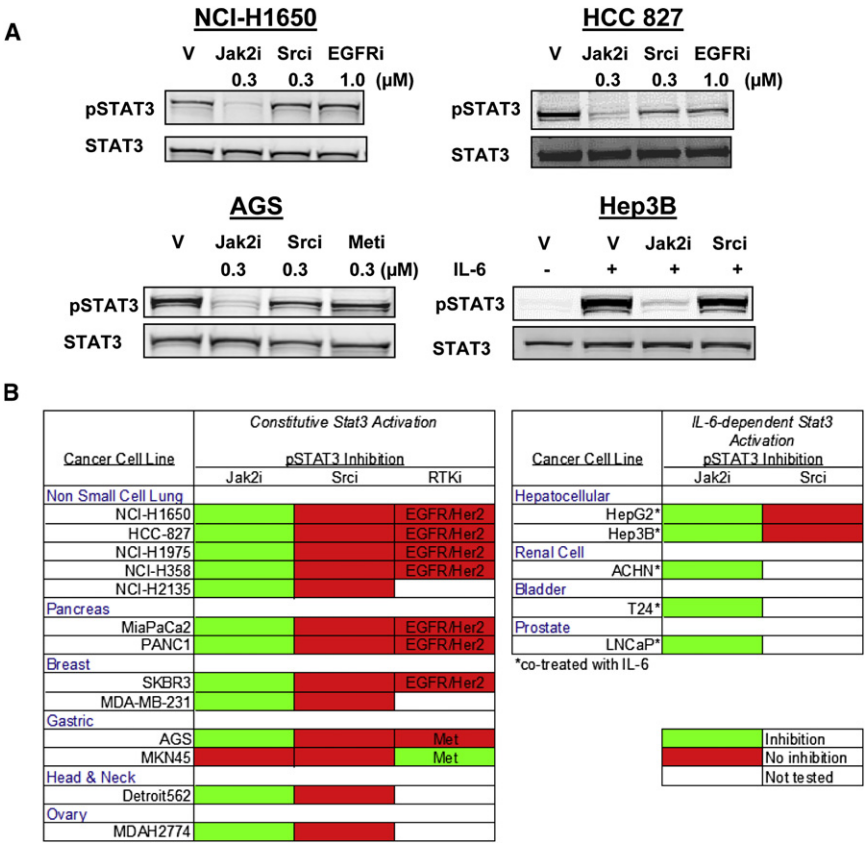

Figure 2. Jak Kinase Inhibition Blocks Stat3 Phosphorylation in a Panel of Human Solid Tumor Cell Lines

Cells were treated with either DMSO (V, vehicle control, 0.01%), Jak2 inhibitor AZ960 (0.3 μM), Src inhibitor Dasatinib (0.3 μM), EGFR inhibitor Gefitinib (1.0 μM), or Met inhibitor PF-2341066 (0.3 μM) for 1 hr and cell lysates were probed for pStat3^{Tyr705} and Stat3 by western blotting.

(A) Representative immunoblots showing decreased pStat3^{Tyr705} in cells treated with a Jak2 inhibitor. Hep3B cells were either stimulated with IL-6 (10 ng/ml) for 30 min or pretreated with the indicated inhibitor for 30 min and then cotreated with IL-6 for an additional 30 min.

(B) Color-coded table of cell lines screened for Stat3 phosphorylation. Drug treatments that resulted in a decrease in Stat3 phosphorylation are shown in green and those which did not modulate pStat3 are shown in red.

line lacking endogenous Stat3 expression and stably expressing a yellow fluorescent protein (YFP)-Stat3 fusion protein (MEF-Stat3-YFP). AZD1480 inhibited Jak2 autophosphorylation in MEF-Stat3-YFP cells when stimulated with oncostatin M (OSM), a member of the IL-6 cytokine family (Hintzen et al., 2008) (Figure 3A). Jak1 activity was also assessed as it is involved in IL-6-stimulated Stat3 activity (Guschin et al., 1995). AZD1480 had no effect on Jak1 autophosphorylation at doses required to inhibit Stat3 phosphorylation (0.5 μM; Figure 3A). Dose-dependent inhibition of Stat3 nuclear translocation was detected with confocal microscopy (Figure 3B) that correlated with inhibition of Jak2 and Stat3 phosphorylation (Figure 3A). The images obtained from confocal microscopy were quantified as described in Experimental Procedures, revealing an IC_{50} for the inhibition of Stat3 nuclear translocation of ~350 nM (Figure 3C).

Jak2 Contributes to Stat3-Mediated Oncogenesis

MEF-Stat3-YFP cells were used as a model of Stat3-mediated oncogenesis to address whether Jak2 inhibition can suppress the growth of a Stat3-dependent tumor. MEF-Stat3-YFP cells have been transformed by the Stat3-YFP fusion construct as

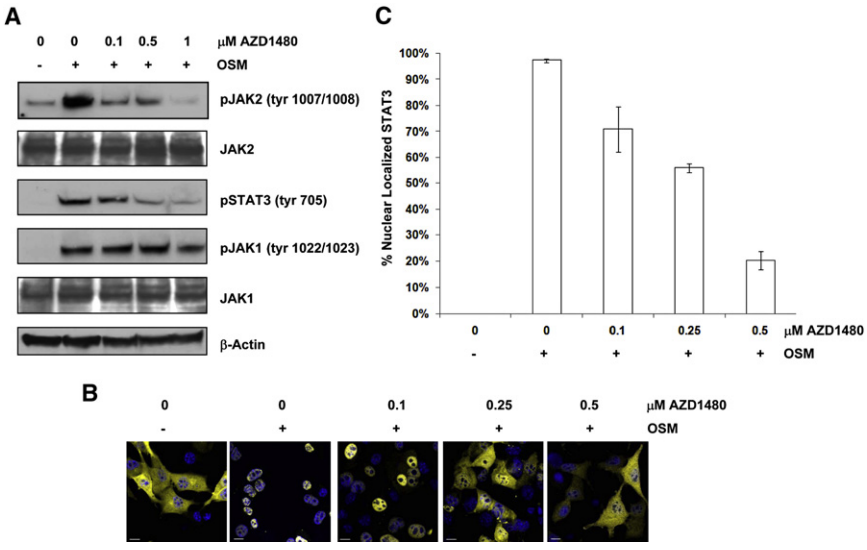

Figure 3. Inhibition of Jak2 Blocks Nuclear Translocation of Stat3

(A) Inhibition of OSM-stimulated Stat3 phosphorylation. Western blot of whole-cell lysates prepared from OSM-stimulated MEF-Stat3-YFP cells treated with the indicated concentrations of AZD1480. Cells were pretreated with AZD1480 for 2 hr, and were then stimulated with 25 ng/ml OSM for 30 min.

(B) Inhibition of Stat3 nuclear translocation. OSM-stimulated MEF-Stat3-YFP cells were treated with the indicated concentrations of AZD1480 and then were stained with DAPI and visualized by confocal microscopy. Blue depicts the nucleus and yellow depicts localization of Stat3 protein. Scale bars represent 10 μm.

(C) Quantification of nuclear translocation of Stat3 of the images in (B); the method is described in the text. Error bars represent SD among the data obtained from five cells in each cohort of the experiment outlined in (B).

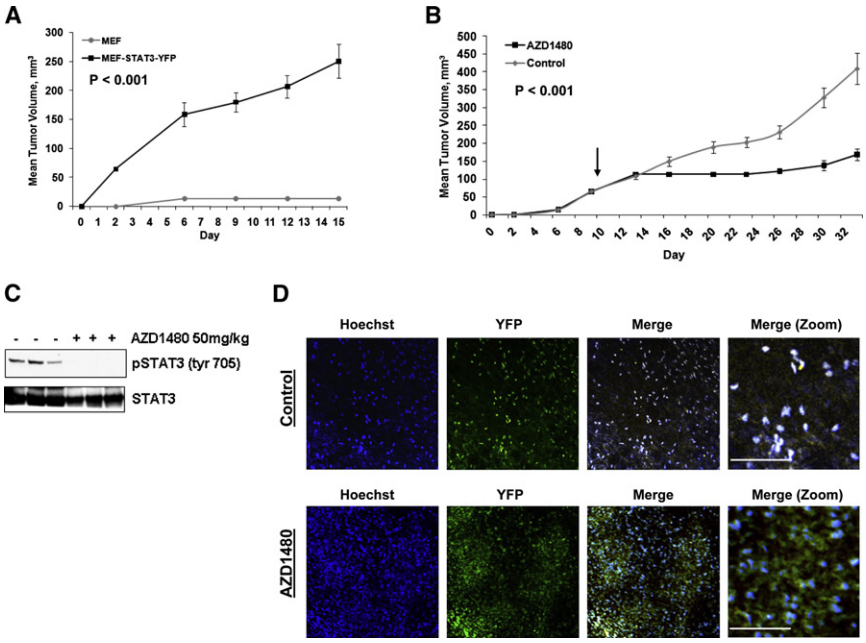

Figure 4. Jak2 Inhibition Suppresses Stat3-Mediated Tumorigenesis

(A) Expression of Stat3 promotes formation of MEF tumors in mice. Tumor growth of MEF cells (gray line) and MEF-Stat3-YFP cells (black line). Results presented as mean tumor volume (n = 8), error bars represent standard error, and the p value (Student's t test) at day 15 is indicated.

(B) Treatment of MEF-Stat3-YFP tumor-bearing mice once daily with 50 mg/kg of AZD1480 (orally) (black line) or vehicle-treated control (gray line). Mice were dosed on a repeating schedule of five continuous days of once daily dosing, followed by 2 days of rest, for 24 days. The arrow indicates initiation of treatment. Results are presented as mean tumor volume (n = 6), error bars represent standard error, and p value (Student's t test) at day 33 is indicated.

(C) AZD1480 inhibits pStat3 activity in MEF-Stat3-YFP tumors. Western blot of tumors following the efficacy study outlined in (B) is shown. Tumors were harvested 2 hr after treatment.

(D) Intravital multiphoton laser microscopy of Stat3 subcellular localization in a tumor. Two photon imaging of intact MEF-Stat3-YFP tumors treated with AZD1480 at 50 mg/kg for 2 weeks, as described above, or with vehicle alone. Tumors were visualized 2 hr after treatment. Stat3 was visualized in real time through exciting the YFP fluorophore tethered to the Stat3 protein. Individual fluorescence channels are presented in the vehicle-treated and AZD1480-treated tumors. Merged images in the control tumor display nuclear localization of Stat3 as depicted by the white dots in the field, created by an overlap of the nuclei and Stat3 emissions. Merged images of the treated tumor depict areas of Stat3 fluorescence that do not overlap with nuclei fluorescence, indicating cytoplasmic localization of Stat3. Scale bars represents 100 μM.

evidenced by their ability to form tumors following subcutaneous implantation in athymic mice, whereas the parental Stat3$^{-/-}$ MEF cells were unable to grow in vivo (Figure 4A). After once daily treatment of tumor-bearing mice with 50 mg/kg AZD1480 (orally), the growth of MEF-Stat3-YFP tumors were inhibited 58% (p = 0.001, n = 6) relative to the vehicle-treated control cohort (Figure 4B).

Stat3 tyrosyl phosphorylation was determined in lysates derived from tumors 2 hr after treatment with AZD1480. Although constitutive Stat3 activity was found in the vehicle-treated tumors, pStat3^{Tyr705} was abolished in tumors that were treated with AZD1480 (Figure 4C). Constitutive phosphorylation of Stat3 in the xenograft setting, but not under routine cell culture conditions (Figure 3A), indicates activation of the pathway likely by the tumor microenvironment.

Intravital multiphoton laser microscopy was performed on mice bearing MEF-Stat3-YFP tumors to visualize Stat3 subcellular localization in the tumors. MEF-Stat3-YFP tumors were found to have a predominance of nuclear-localized Stat3 coinciding with the constitutive expression of pStat3^{Tyr705} observed by western blotting (Figure 4D). Treatment of MEF-Stat3-YFP tumors with AZD1480 resulted in inhibition of Stat3 nuclear translocation in vivo, correlating with the inhibition of pStat3^{Tyr705} observed after treatment with AZD1480 (Figure 4D).

Jak2 Mediates IL-6-Dependent Survival of Androgen-Independent Prostate Cancer Cells

The LnCaP subline LN-17 expresses constitutive Stat3 activity as a consequence of stable expression of an exogenous IL-6 gene and endogenous expression of the IL-6R (Lee et al., 2003; Lou et al., 2000). The resulting IL-6 autocrine loop allows LN-17 cells to survive under androgen deprivation conditions. LN-17 cells were treated with AZD1480 to determine whether Jak2 blockade can abrogate IL-6-dependent survival. Dose-dependent inhibition of pStat3^{Tyr705} (Figure 5A) and Stat3 DNA binding activity (Figure 5B) was observed in response to the addition of AZD1480, as was a loss of viability (Figure 5C). The loss of viability was associated with a dose-dependent increase in the apoptotic markers Annexin V (Figure 5D) and PARP cleavage (85 kDa fragment) (Figure 5E). To confirm the Jak2 dependency of Stat3 signaling in these cells, we tested the effect of two siRNAs directed against Jak2 to determine whether they could inhibit Stat3 tyrosine phosphorylation. Reduction of Jak2 protein expression by siRNAs 1 and 2 inhibited Stat3 signaling compared to a nonsilencing control siRNA (Figure 5F).

AZD1480 Suppresses the Growth of Tumors with Constitutive Stat3 Activity

The LN-17 subline was incapable of growth in mice, thus we were unable to assess the in vivo efficacy of Jak2 inhibition in this model. To determine whether AZD1480 could impact the growth of human tumors, we turned to solid tumor xenograft lines that displayed constitutive Stat3 activation and an IL-6 autocrine loop. The cancer cell lines DU145 (prostate), MDAH2774 (ovarian), and MDA-MB-468 (breast) were chosen. DU145 and MDA-MB-468 express IL-6 autocrine loops (Berishaj et al., 2007; Okamoto et al., 1997), and we have determined that MDAH2774 cells both secrete IL-6 and express IL-6R (Figure 6A). Constitutive pStat3^{Tyr705} was inhibited in a dose-dependent manner by AZD1480 in all three cell lines (Figure 6B). Significant inhibition of pStat3^{Tyr705} is observed at 0.1 μM drug

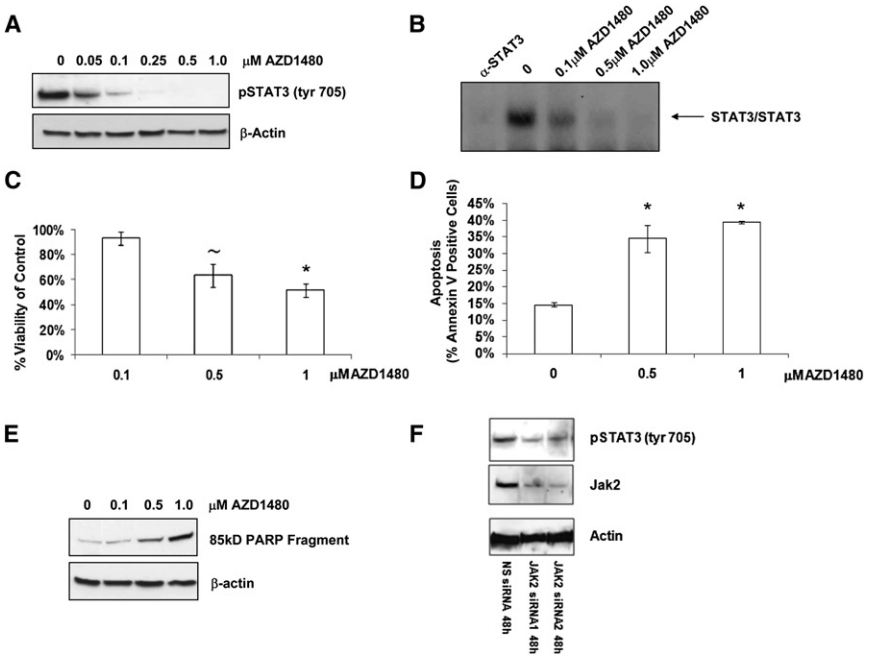

Figure 5. Jak2 Mediates IL-6-Dependent Survival in Human Prostate Cancer Cells

(A) Stat3 activity was assayed by western blotting in LN-17 cells treated for 24 hr with the indicated concentrations of AZD1480.

(B) EMSA to visualize Stat3 DNA binding after treatment with a Jak2 inhibitor. LN-17 cells were treated as in (A) and EMSA was performed to monitor Stat3 homodimer DNA binding activity. The first lane is the control-treated sample incubated with a Stat3 blocking antibody to confirm Stat3 binding.

(C) Cell viability was assayed with an MTS assay 72 hr after treatment with the indicated concentrations of AZD1480. Error bars represent the SD of three experiments conducted independently. $\sim p < 0.02$, $^{*}p < 0.01$.

(D) Flow cytometric analysis of LN-17 cells stained with Annexin V 72 hr after treatment with the indicated concentrations of AZD1480. Error bars represent the SD among triplicate samples. $^{*}p < 0.01$.

(E) Apoptosis was assayed by western blot with an antibody against the cleaved 85 kDa PARP fragment in LN-17 cells treated with the indicated concentrations of AZD1480 for 72 hr.

(F) Two siRNAs (300 nM) targeting Jak2 were transfected with the Amaxa Nucleofector system and were harvested 48 hr later. Cell lysates were immunoblotted with indicated antibodies. A nonsilencing (NS) siRNA was used as a negative control.

and near ablation of signal is observed at 0.25–0.5 μM. These cell lines show greater sensitivity to inhibition of Stat3 phosphorylation by AZD1480 than does the MEF-Stat3-YFP line (Figure 3A), perhaps reflecting Stat3 overexpression in the transfected MEF cells. In all three lines, exogenous addition of IL-6 induced phosphorylation of Stat3^{Tyr705} (Figure 6C), which was inhibited following treatment with AZD1480.

We transfected siRNAs directed against Jak1, Jak2, and Tyk2 to identify the Jak family kinase primarily responsible for Stat3 activation in MDAH2774 cells. While we observed successful inhibition of Jak1, Jak2, and Tyk2 protein expression with the siRNAs, only reduction of Jak1 protein suppressed Stat3 phosphorylation compared to the GAPDH negative control siRNA (Figure 6D).

AZD1480 did not inhibit in vitro growth of DU145, MDAH2774, and MDA-MB-468 cells at doses that abrogated Stat3 tyrosyl phosphorylation (data not shown). In a 72 hr viability assay, GI_{50} values for the three lines ranged from 2.4 to 5.4 μM, indicating that under standard cell culture conditions, Jak2/Stat3 signaling was not essential for survival and growth inhibition probably reflects off-target activities manifested at the high drug levels. Similar observations are made for the panel of solid tumor cell lines shown in Figure 1B. To assess the impact of Jak inhibition on in vivo tumor growth, we treated mice bearing DU145 and MDA-MB-468 tumors once daily with AZD1480. In this context, AZD1480 demonstrated significant tumor growth inhibition of DU145 (81% growth inhibition, $p < 0.001$, $n = 7$) and MDA-MB-468 (111% growth inhibition, $p < 0.001$, $n = 7$) xenografts, relative to vehicle-treated cohorts (Figure 7A).

An alternative dosing schedule and dose levels were tested in mice bearing MDAH2774 xenografts. Tumor-bearing mice were treated with 1, 10, and 30 mg/kg AZD1480 twice daily. A dose-dependent reduction in tumor growth was observed, with comparable tumor growth inhibition observed at 10 mg/kg twice daily (71% growth inhibition, $p < 0.001$, $n = 10$) to that observed at 50 mg/kg once daily. Upon twice daily dosing with 30 mg/kg AZD1480 (Figure 7A), tumor regression was observed (139% growth inhibition, $p < 0.001$, $n = 10$). No lethal toxicity or weight loss was observed at the doses of AZD1480 spanning 26 days of dosing (Figure S4). Given the well established role of Jak family kinases in hematopoiesis, and particularly of Jak2 in erythropoiesis, we evaluated red and white blood cell counts in mice treated with AZD1480. No significant changes in white blood cell counts occurred after 10 days of treatment at 10 or 30 mg/kg twice daily. Over the same time period red blood cell counts decreased approximately 13% in response to 30 mg/kg twice daily AZD1480, while no changes were observed at 10 mg/kg twice a day (Figure S5).

Tumor Growth Inhibition Correlates with Inhibition of Constitutive Stat3 Signaling

Complete inhibition of pStat3^{Tyr705} was observed in tumor lysates prepared from xenografts harvested 2 hr after AZD1480 treatment (Figure 7B). More detailed kinetic analysis of tumor lysates from MDAH2774 xenograft-bearing mice 2, 6, 10, and 16 hr after a single 30 mg/kg dose of AZD1480 demonstrated that expression of pStat3^{Tyr705} begins to recover by 6–10 hr after drug treatment and appears to be fully recovered by 16 hr (Figure 7B). Immunohistochemical analysis of tumor sections demonstrated that pStat3^{Tyr705}, and its inhibition by AZD1480, was evident not only in tumor cells but also in adjacent mouse tumor stroma (Figure S6).

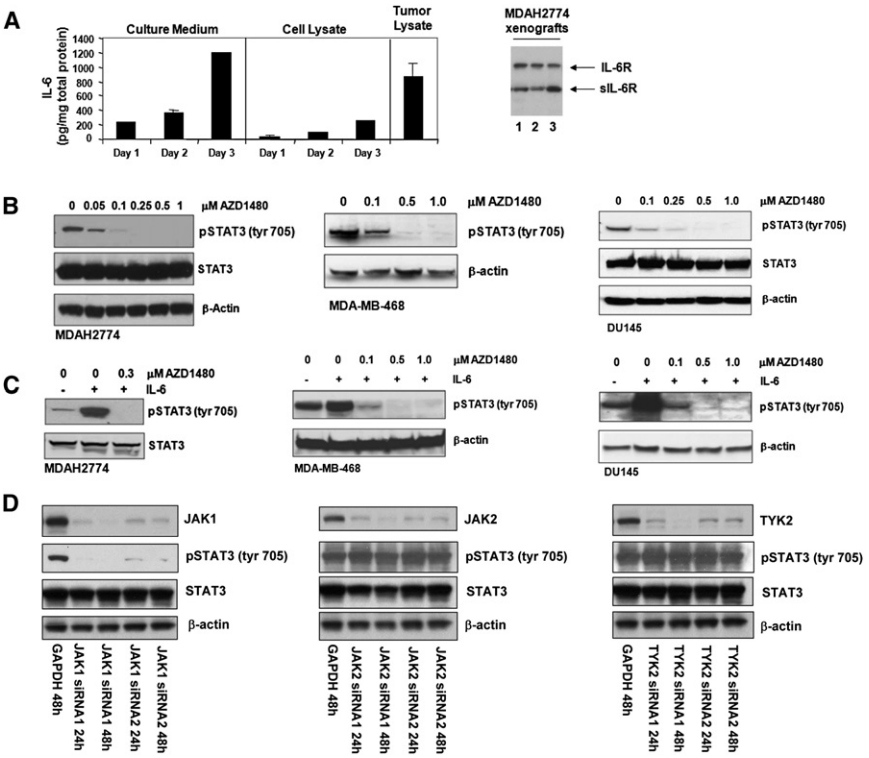

Figure 6. Jak Kinase Inhibition Abrogates IL-6-Induced and Constitutive Stat3 Activity of Human Cancer Cells

(A) MDAH2774 cells express IL-6 and IL-6R. Culture medium and cell lysates were collected from MDAH2774 cells after 1, 2, and 3 days of culture, and tumor lysates were collected from mice bearing MDAH2774 xenografts (n = 7). Human IL-6 was measured by Luminex Immunoassay using the Milliplex cytokine kit (Millipore). For culture medium and cell lysate, error bars denote the SD for each sample measured in duplicate. For tumor lysate, samples were measured in triplicate and the error bar denotes the SD of the mean measurements. IL-6R was assayed in three individual tumor lysates by western blotting.

(B) AZD1480 inhibits constitutive Stat3 activity in human cancer cells. Western blotting of whole-cell lysates of DU145, MDA-MB-468, and MDAH2774 cells prepared 2 hr after treatment with the indicated concentrations of AZD1480 is shown.

(C) Western blot analysis of whole cell lysates prepared from DU145, MDA-MB-468, and MDAH2774 cells that were starved in 5% CS-FBS for 18 hr (DU145 and MDA-MB-468) or serum starved for 3 hr (MDAH2774), and then treated with the indicated concentrations of AZD1480 for 2 hr. Cells were then stimulated with 10 ng/ml IL-6 for 15 min after pretreatment with AZD1480.

(D) Jak1 siRNA blocks phosphorylation of Stat3 in MDAH2774 cells. Jak1-siRNAs, Jak2-siRNAs, or Tyk2-siRNAs (100 nM) were transfected into MDAH2774 cells using the Amaxa Nucleofector system and were harvested 24 and 48 hr later. Cell lysates were immunoblotted with indicated antibodies. GAPDH siRNA was used as a negative control.

IL-6 can also stimulate the ERK and PI3K pathways (Culig et al., 2005); therefore, we examined whether Jak inhibition was modulating these signaling pathways. No significant change in expression of p44/42 pMAPK and pAKT^{Ser473} was detected in tumors treated with AZD1480 compared to control animals (Figure 7B). Furthermore, since AZD1480 inhibited Aurora A enzyme activity in the kinase panel (Figure S2), xenograft tumor sections were examined for evidence of mitotic block, the

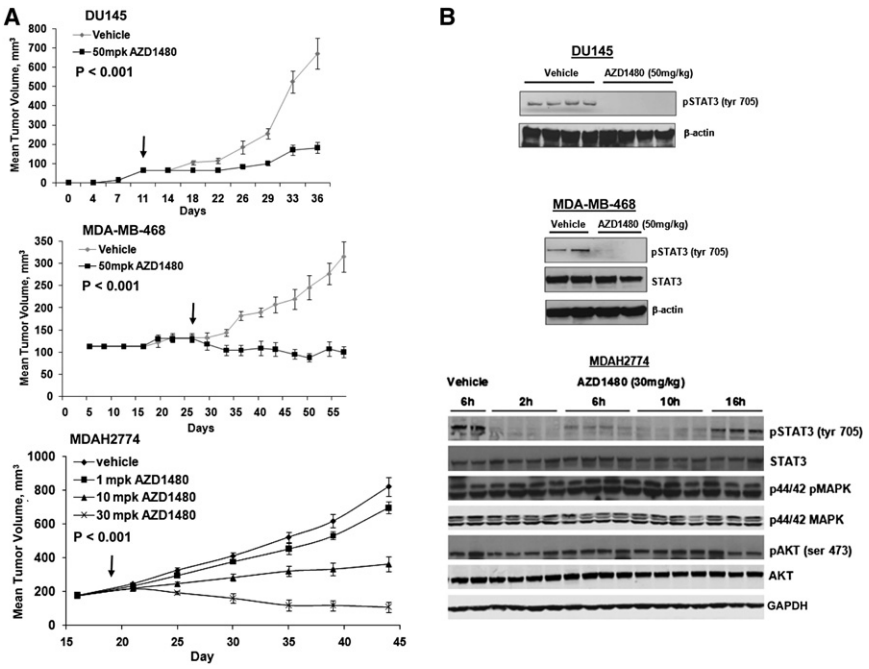

Figure 7. AZD1480 Suppresses the Growth of Human Xenograft Tumors Harboring Constitutive Stat3 Activity

(A) DU145 and MDA-MB-468 tumor-bearing mice were treated once daily with AZD1480 (black line) at 50 mg/kg (orally) or vehicle (gray line) for 5 days, followed by 2 days of rest, over a total course of treatment of 26 days (DU145) or 30 days (MDA-MB-468). The arrow indicates initiation of treatment. Results are presented as mean tumor volume (n = 7), bars indicate standard error, and p value (Student's t test) at day 37 (DU145) or day 57 (MDA-MB-468) is indicated. As shown on the bottom, MDAH2774-bearing mice were treated twice daily with 1, 10, and 30 mg/kg (orally) for 26 consecutive days. The arrow indicates initiation of therapy. Results presented as mean tumor volume, bars indicate standard error, and p value (Student's t test) at day 44 is indicated.

(B) Western blot analysis of tumors 2 hr after treatment with AZD1480. DU145 tumors were obtained after 26 days of treatment with 50 mg/kg AZD1480, MDA-MB-468 tumors were obtained after 30 days of treatment with 50 mg/kg AZD1480, and MDAH2774 tumors were exposed to only a single dose of 30 mg/kg AZD1480.

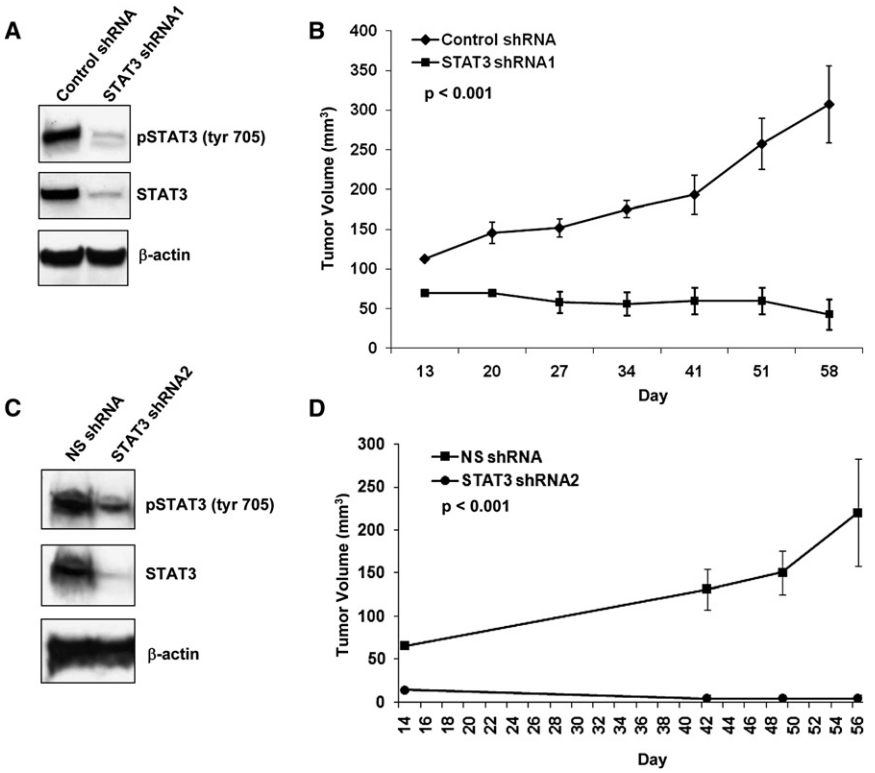

Figure 8. Expression of Stat3 shRNA Inhibits the Growth of Human Breast Cancer Cells

(A) Western blot of whole-cell lysates derived from MDA-MB-468 cells grown in culture expressing Stat3 shRNA1 or vector alone.

(B) Reduction of Stat3 expression results in inhibition of MDA-MB-468 tumor growth. The growth of MDA-MB-468 subcutaneous xenografts expressing either Stat3 shRNA1 or vector alone control were monitored for 58 days. Results are presented as mean tumor volume (n = 6) with standard error, and p value (Student's t test) at day 58 is indicated.

(C) Western blot of whole-cell lysates derived from MDA-MB-468 cells grown in culture expressing Stat3 shRNA2 or nonsilencing (NS) control shRNA.

(D) The growth of MDA-MB-468 subcutaneous xenografts expressing either Stat3 shRNA2 or nonsilencing shRNA were monitored for 56 days. Results are presented as mean tumor volume (n = 6) with standard error, and p value (Student's t test) at day 56 is indicated.

phenotypic endpoint of Aurora A inhibition (Manfredi et al., 2007), by staining for the mitotic marker pHisH3. No modulation of pHisH3 staining was observed in MDAH2774 xenografts treated with 30 mg/kg AZD1480 for up to 16 hr after the dose was given (Figure S7).

To confirm that suppression of tumor growth observed upon AZD1480 treatment was due to inhibition of Stat3 signaling, we created MDA-MB-468 cells stably expressing either Stat3 shRNA or vector alone. MDA-MB-468 cells expressing Stat3 shRNA displayed significant decreases in both total Stat3 and $pStat3^{Tyr705}$ in culture compared to empty vector or non-silencing control shRNA-expressing cells (Figures 8A and 8C). In vitro evaluation of the stably infected MDA-MB-468 cells revealed no significant change in the growth of Stat3 shRNA-expressing compared to empty vector cells (data not shown). However, the growth of MDA-MB-468 tumors expressing Stat3 shRNAs were significantly impaired compared to tumors expressing the empty vector or non-silencing shRNA (Figures 8B and 8D).

The converse experiment to inhibiting Stat3 expression is overexpression of an activated Stat3 mutant whose activity is independent of tyrosine phosphorylation. To confirm that tumor growth inhibition observed upon treatment with AZD1480 was due to inhibition of Stat3 signaling, we tested whether AZD1480 could inhibit the growth of 786-0 renal cell carcinoma xenografts expressing a constitutively active Stat3 mutant, Stat3C (Bromberg et al., 1999). While 786-0 xenografts expressing Stat3C exhibited no growth inhibition, the growth of vector control xenografts were inhibited following 41 days of treatment with 50 mg/kg AZD1480 when compared to vehicle-treated xenografts (48% growth inhibition, p = 0.038, n = 10) (Figure S8). Moreover, decreased apoptosis was observed after treatment with AZD1480 in Stat3C-expressing xenografts compared to treated control cells (Figure S8). These data provide further evidence that tumor growth inhibition by AZD1480 is due at least in part to inhibition of Stat3 signaling.

DISCUSSION

Persistent Stat3 activation is prevalent in many types of human cancers and contributes to tumor progression. While direct inhibition of transcription factors with small-molecule inhibitors has proven challenging, targeting of upstream activating kinases offers a pharmaceutically viable alternative. The mechanism of persistent Stat3 activation in cancer tissues and cell lines has been attributed to phosphorylation by Jak and Src family kinases, as well as activated receptor tyrosine kinases including EGFR (Boccaccio et al., 1998; Bowman et al., 2000; Lo et al., 2007; Quesnelle et al., 2007). The availability of Jak2 inhibitors such as AZD1480 makes it possible to test the impact of Jak inhibition on Stat3 activation in solid tumor cell lines. In a panel of cell lines displaying constitutive Stat3 activation, we found that almost all cell lines were dependent on Jak kinase activity for Stat3 activation.

In none of the cell lines tested was tyrosyl phosphorylation of Stat3 suppressed by inhibition of Src activity, and in only one cell line was Stat3 found to be phosphorylated downstream of a receptor tyrosine kinase, in this case c-Met. While previous reports have indicated a role for Src family kinases and growth factor receptors such as EGFR in phosphorylation of Stat3, it is likely that these receptor and non-receptor tyrosine kinases cooperate with Jak family kinases to activate Stat3 (Gao et al., 2007; Garcia et al., 2001; Niu et al., 2002a; Wang et al., 2000; Xi et al., 2003). Thus, depending on the cellular context, other non-receptor and receptor tyrosine kinases may indirectly

activate Stat3 through Jak family kinases. Importantly, our data demonstrate that Jak family kinases are essential for Stat3 activation. These observations indicate that Jak-mediated phosphorylation and activation of Stat3 is a common mechanism in a majority of human cancer cell lines.

Inhibition of Stat3 phosphorylation by AZD1480 in MEF-Stat3-YFP cells correlates with dose-dependent inhibition of Stat3 nuclear translocation and Stat3-dependent tumor growth. Reconstitution of Stat3 expression in MEF cells resulted in tumor growth, in contrast to the parental Stat3 null cells, confirming the essential role of Stat3 in this tumor model. In vivo activation of Stat3 appears to be primarily mediated by Jak2, since treatment of tumor-bearing mice with AZD1480 resulted in inhibition of Stat3 activation and tumor growth. We also demonstrate Stat3 subcellular localization in MEF-Stat3-YFP tumors by intravital multiphoton laser microscopy.

In cancer cell lines and tissues, there is evidence for constitutive activation of Stat3 through chronic cytokine stimulation upon the establishment of autocrine or paracrine loops, often involving IL-6 (Culig et al., 2005; Grivennikov and Karin, 2008; Rabinovich et al., 2007). The IL-6R shares the common gp130 subunit that signals through receptor-associated Jak family kinases. We have shown, in multiple cell lines, that IL-6-driven stimulation of Stat3 tyrosyl phosphorylation can be completely blocked by AZD1480. IL-6 is known to signal through Jak1, Jak2, and Tyk2, with Jak1 reported to play an essential role (Guschin et al., 1995). We observed only slight inhibition of pJak1$^{Tyr1007/1008}$ at drug concentrations sufficient to inhibit pStat3^{Tyr705} in MEF-STAT3-YFP cells stimulated by the IL-6 family cytokine OSM. However, given the comparable potency of AZD1480 for Jak1 at high ATP concentrations in vitro, and that siRNA targeting Jak1 led to a reduction of Stat3 activity in tumor cells, we cannot rule out the possibility that inhibition of pStat3^{Tyr705} might be dependent on inhibition of both Jak1 and Jak2 activity.

DU145, MDA-MB-468, and MDAH2774 express IL-6 autocrine loops (Berishaj et al., 2007; Okamoto et al., 1997) and their tumorigenesis was inhibited upon treatment with AZD1480. After once daily treatment with 50 mg/kg AZD1480, growth of DU145 and MDA-MB-468 xenografts were inhibited. Comparable tumor growth inhibition was seen in MDAH2774 xenografts dosed twice daily at 10 mg/kg. Increasing the twice-daily dosing level to 30 mg/kg resulted in tumor regression. We found Jak inhibition to be well tolerated at the doses and schedules described. However, given the role of Jak family kinases in hematopoiesis, more prolonged or intensive treatment may require optimization of dose and/or schedule to achieve efficacy with manageable impact on hematopoiesis.

Pharmacodynamic analysis of Stat3 phosphorylation demonstrated significant inhibition of pStat3 for >10 hr after a single dose of 30 mg/kg AZD1480. Coupled with the anti-tumor efficacy data, this suggests that optimal tumor growth inhibition correlates with sustained Stat3 pathway signaling inhibition over a 24 hr period. Reduction of Stat3 expression with shRNA in MDA-MB-468 xenografts significantly inhibited tumor growth. Introduction of a constitutively active Stat3C mutant into 786-0 xenografts caused these tumors to become resistant to AZD1480 treatment. These findings further support the conclusion that tumor growth inhibition observed upon treatment with AZD1480 is dependent at least in part on inhibition of Stat3 signaling.

Notably, no inhibition of growth was observed in cell culture for any of the xenograft cell lines at doses of AZD1480 that maximally inhibited Stat3 phosphorylation. In addition, shRNA-mediated knockdown of Stat3 did not significantly affect the growth of MDA-MB-468 cells in vitro. One possibility for this discrepancy is that Jak/Stat signaling is not required for growth in standard two-dimensional cell culture in which cells are exposed to the multitude of growth factors present in serum. In the in vivo setting, the increased complexity of the tumor microenvironment could provide a context in which Jak/Stat activity is essential for survival. This could manifest as a tumor-autonomous dependence on Jak/Stat signaling and/or a dependence on Jak/Stat signaling in the tumor microenvironment. Using IHC analysis of tumor xenografts, we have demonstrated activation of Stat3 in the tumor stroma in addition to tumor cells and inhibition of both signals following treatment with AZD1480. These observations raise the possibility that tumor growth inhibition may be mediated, at least in part, by blockade of stromal Stat3 activity.

Aberrant activation of Stat3 has been extensively documented in human cancers and a preponderance of clinical and preclinical data have supported a role for Stat3 in promoting tumorigenesis (Yu and Jove, 2004). Evidence has more recently been provided for chronic cytokine stimulation being a feature of some tumors with constitutive Stat3 phosphorylation, providing a mechanistic rationale for pathway activation (Grivennikov and Karin, 2008). It remains to be determined why Stat3 activation in tumor cells is not subject to the negative feedback regulation present in normal cells. The role of Jak family kinases as the catalytic subunits of cytokine receptors positions them as attractive therapeutic targets for pathway inhibition. Recent development of Jak2 inhibitors for myeloproliferative neoplasms provides the means of testing Jak kinase as a therapeutic target in solid tumors. Our data demonstrate that Stat3 activation is primarily mediated by Jak kinase activity in a wide range of solid tumor cell lines and that Jak inhibition can suppress the growth of tumors with constitutive Stat3 activation. These data validate Jak kinase as a molecular target in tumor indications beyond myeloproliferative neoplasms and support the development of Jak inhibitors for treatment of human solid tumors harboring persistent Stat3 activity.

EXPERIMENTAL PROCEDURES

Reagents

AZD1480, a 4-(Pyrazol-3-ylamino) pyrimidine derivative, and AZ960 were synthesized by AstraZeneca. Gefitinib (AstraZeneca), Dasatinib (BMS-354825; Bristol-Myers Squibb Oncology), and PF-2341066 (Pfizer) were also used in these studies. Stock solutions were diluted in dimethylsulfoxide (DMSO; Sigma-Aldrich) and then diluted in culture medium for use. Anti-pStat3 (Y705), anti-Stat3, anti-Stat5, anti-pJak2 (Y1007/1008), anti-Jak2, anti-pJak1 (Y1022/1023), anti-Jak1, anti-phospho-p44/42 MAPK, anti-p44/42 MAPK, anti-pAKT, anti-AKT, anti-pEGFR (Tyr1068), anti-pSrc family (Tyr416), anti-GAPDH, and anti-cleaved PARP were purchased from Cell Signaling Technology. Anti-pStat5 (Tyr694) was purchased from BD Biosciences. HRP-conjugated anti-mouse, HRP-conjugated anti-rabbit, and HRP-conjugated anti-goat antibodies were obtained from Cell Signaling Technology or Santa Cruz Biotechnology. Anti-β-actin was obtained from Sigma-Aldrich. IRDye 680 goat anti-mouse and IRDye 800CW goat anti-rabbit antibodies were obtained from Li-Cor. IL-6 and goat anti-soluble IL6-receptor antibody were purchased from R&D Systems.

Cell Lines

The Ba/F3 engineered cells were generated and maintained as previously described (Gozgit et al., 2008). MEF-Stat3-YFP cells were generated as previously described (Herrmann et al., 2004) and maintained in Dulbecco's modified Eagle's medium (DMEM) supplemented with 10% heat-inactivated FBS, 100 U/ml penicillin, and 0.1 mg/ml streptomycin (GIBCO). LN-17 cells (Lee et al., 2003) (a gift from A. Gao) were maintained in RPMI-1640 supplemented with 10% heat-inactivated FBS, 100 U/ml penicillin, 0.1 mg/ml streptomycin, (GIBCO), and 0.4 mg/ml G418. MDA-MB-468-STAT3-shRNA cells and the corresponding vector alone control cells were maintained in DMEM supplemented with 10% heat-inactivated FBS (100 U/ml) and 1.5 μg/ml puromycin. 786-0 Stat3C and vector-expressing control cells were generated as previously described (Xin et al., 2009) and maintained in RPMI-1640 supplemented with 10% heat-inactivated FBS, 100 U/ml penicillin, 0.1 mg/ml streptomycin, and 0.5 mg/ml G418. All other cell lines were obtained from ATCC and maintained according to their recommendations.

Enzyme Assays and Kinase Profiling

Inhibition studies of AZD1480 were performed using recombinant Jak1 (amino acids 850–1154; Carna Biosciences Inc.), Jak2 (amino acids 808–1132; Millipore), or Jak3 (amino acids 781–1124; AstraZeneca R&D Boston) under buffer conditions of 50 mM HEPES (pH 7.3), 1 mM DTT, 0.01% Tween-20, 50 μg/ml BSA, and 10 mM $MgCl_2$. Jak3 enzyme was expressed as N-terminal GST fusion in insect cells and purified by glutathione affinity and size-exclusion chromatographies. Enzymes were assayed in the presence of AZD1480 (10 point dose response, in triplicate, from 8.3 μM to 0.0003 μM in half-log dilution steps) using 1.5 μM peptide substrate (Jak1: FITC-C6-KKHTDDG YMPMSPGVA-NH2; Intonation Technologies Inc.; Jak2 and Jak3: FAM-SRCtide; Molecular Devices) and screened under their respective ATP K_m (Jak1: 55 μM, Jak2: 15 μM, Jak3: 3 μM) and approximated physiological ATP concentration of 5 mM. Phosphorylated and unphosphorylated peptides were separated and quantified by a Caliper LC3000 system (Caliper Life Sciences) for calculating percent inhibition. Jak2 kinetic studies were performed as previously described (Gozgit et al., 2008).

Viral Vector Production

293T cells were plated at a density of 4×10^6 cells per 10 cm culture dish. Cells were cotransfected by calcium phosphate coprecipitation with either 15 μg of pLKO1-Stat3 shRNA1 (#840) or pLKO1-Stat3 shRNA2 (#842) or pLK01-puro or pLK01-non-silencing shRNA (Sigma-Aldrich) and 10 μg of pPACK packaging plasmid mix (SBI). The culture medium was replaced with fresh medium after 6 hr. Supernatant was collected 24 and 48 hr after transfection. For determining the viral titers, 105 HT1080 cells were seeded in a six-well plate and transduced with various dilutions of the vector in the presence of 4 μg of Polybrene per milliliter (Sigma-Aldrich). The culture medium was replaced 48 hr later with fresh medium containing puromycin (Sigma-Aldrich) at a concentration of 1.5 μg/ml. Puromycin-resistant colonies were counted 10 days after transduction. MDA-MD-468 cells were transduced with viral vector at a multiplicity of infection of 0.5.

Luminex Immunoassay

IL-6 was measured with the human-specific Milliplex map kit (Millipore Corporation) in accordance with the manufacturer's instructions and the Luminex 100 System (Bioplex System; Bio-Rad). Samples were assayed in duplicate for cell culture medium and cell lysate and in triplicate for tumor lysate. Total protein (mg/ml) was determined with a BCA protein assay kit (Thermo Scientific).

Immunohistochemistry

MDAH2774 xenograft tissues were harvested 2 and 6 hr after a single 30 mg/kg dose of AZD1480, fixed in 10% neutral-buffered formalin (24 hr), paraffin embedded, and sectioned (5 μm). Immunohistochemistry was performed on the Ventana Discovery XT Autostainer using the standard CC1 protocol. Primary antibodies were pStat3 antibody (Cell Signaling Technology), total Stat3 (Cell Signaling Technology), and pHisH3 (Cell Signaling Technology) with either the OmniMap DAB detection kit or the DABMap detection kit. Secondary antibody was a biotinylated anti-rabbit IgG (Vector Laboratories) used per manufacturer's instructions. A negative control reagent, nonimmune rabbit Ig (Ventana), was run in place of primary antibody to evaluate nonspecific staining. The slides were counterstained with hematoxylin (Ventana).

Confocal Microscopy

For confocal microscopy, cells were fixed with formaldehyde as described previously (Herrmann et al., 2004), and then mounted with Vectashield HardSet mounting medium with DAPI (Vector Laboratories). Confocal imaging was carried out on an LSM 510 Meta confocal microscope (Zeiss; 63×, 1.2 NA Zeiss water immersion objective, 1 μM confocal slice). YFP emissions were detected as previously described (Pranada et al., 2004). DAPI was visualized with a two-photon laser exciting at 435–485nm.

Quantification of Stat3 Nuclear Translocation

YFP fluorescence intensity acquired by linear profiles with LSM image browser were corrected and normalized and used for calculating a translocation index (T_i) of Stat3 with the equation $T_i = 1 - (cyt_{xmin}/nuc_{xmin}) \times (nuc_{0min}/cyt_{0min})$, where cyt_{0min} and nuc_{0min} are the average cytoplasmic and nuclear YFP fluorescence, respectively, in unstimulated cells. Average cytoplasmic and nuclear fluorescence of YFP in stimulated cells are cyt_{xmin} and nuc_{xmin}, respectively. Error bars represent the SEM of five cells/cohort.

Intravital Multiphoton Laser Microscopy

Mice were maintained under specific pathogen-free conditions and were used in compliance with protocols approved by the Institutional Animal Care and Use Committees of City of Hope, which conform to institutional and national regulatory standards on experimental animal usage. Mice were anesthetized with isofluorane gas, kept warm with either a heat lamp or a heating blanket, and prepared for surgery. Mice were then retro-orbitally injected with 25 μg of Hoechst 33342 (Sigma-Aldrich) and 10 μG of Annexin V-FITC (BioVision) in Hank's balanced salt solution. An incision was made near the midline, creating a skin flap that exposed the tumor that was then folded over and pinned to the cork surface of the microscope stage insert. The imaging site was cleaned with normal saline and ddH2O and then coverslipped. The coverslip was held in place against the tumor tissue with thumbscrews. The mouse continued to receive isofluorane anesthesia while imaging was performed utilizing Prairie Technologies Ultima microscope with illumination from a Coherent Chameleon Ultra II Ti:Sapphire laser. An Olympus 10×/0.3 objective lens was used and the excitation and emission spectra used for the fluorophores were as follows: Hoechst 33342 excitation at 730 nm with emission between 435 and 485 nm and Annexin V-FITC and YFP excitation at 860 nm with emission between 500 and 550 nm. Extracellular matrix is given by second harmonic generation through $\lambda_{[excit.]} = 890$ nm. TIFF-formatted images were collected using Prairie View software at a resolution of 1024 × 1024 pixels and then transferred to Image Pro software version 6.3 for brightness, contrast, and color adjustment.

Western Blotting

Cells were lysed with SDS buffer or RIPA buffer. Xenograft lysates were prepared by FastPrep homogenization (MP Biomedicals) in Swedish lysis buffer (20 mM Tris [pH 7.5], 150 mM NaCl, and 1% NP40) or RIPA buffer, supplemented with 1× protease (Roche) and phosphatase (Sigma-Aldrich) inhibitors. 50–100 μg of protein were resolved in 4%–12% SDS-PAGE or NuPage Novex gels (Invitrogen) and transferred to NuPage nitrocellulose membranes (Invitrogen). After blocking (1 hr at room temperature) with 5% milk in PBS-0.1% Tween 20, membranes were incubated overnight with indicated antibodies and then exposed to secondary antibody. Immunoreactive proteins were visualized with an enhanced chemiluminescence detection system (Pierce Biotechnology). Signals were also detected with the Li-Cor Odyssey Infrared system using Li-Cor blocking buffer and fluorescent Li-Cor secondary antibodies. The westerns and quantitation described with the Ba/F3 engineered cells were performed as previously described (Gozgit et al., 2008).

Cell Viability Assays

The Ba/F3 engineered cells were assayed as previously described (Gozgit et al., 2008). Cell growth in vitro was measured using the CellTiter 96 AQ Nonradioactive cell proliferation assay (Promega). In brief, LN-17 cells (5×10^3) were plated in 96-well plates in quintuplicate in RPMI plus 10% charcoal-stripped FBS and allowed to attach for 24 hr prior to the addition of DMSO or AZD1480 to the culture medium. After 72 hr, 20 μl/well of

3-(4,5-dimethylthiazol-2-yl)-5-(3-carboxymethoxyphenyl)-2-(4-sulfophenyl)-2H-tetrazolium/phenazine ethosulfate solution was added. After incubation (1 hr, 37°C, 5% CO_2 atmosphere), absorbance at 490 nm was recorded by using an ELISA plate reader.

Flow Cytometric Analysis of Annexin V

LN-17 cells (2×10^5) were seeded into six-well dishes and allowed to attach overnight. Following attachment, the medium was replaced with RPMI containing 10% charcoal-stripped FBS with DMSO, or AZD1480 as indicated. After 72 hr incubation, cells were washed twice with cold PBS, harvested with PBS supplemented with EDTA, and stained with the Annexin-V-FITC apoptosis detection kit (BD Biosciences) according to the manufacturer's instructions. Data acquisition and analysis was performed by the Flow Cytometry Core Facility at the City of Hope.

EMSA

For the detection of DNA-binding activity of Stat3 by EMSA, nuclear protein extracts were prepared using high-salt extraction as previously described (Garcia et al., 2001). For detection of Stat3 DNA-binding activity, 5 μg of nuclear protein from AZD1480-treated LN-17 cells were incubated with ^{32}P-radiolabeled double-stranded DNA oligonucleotides using a high-affinity variant of the sis-inducible element derived from the c-*fos* gene promoter, which binds activated Stat3 and Stat1 proteins (Wagner et al., 1990; Yu et al., 1995). Anti-Stat3 polyclonal antibodies (C20X; Santa Cruz Biotechnology) were used as blocking antibodies for Stat3 binding identification. For blocking assays, 1 ml of the concentrated Stat3 antibody was pre-incubated with nuclear protein for 20 min at room temperature prior to the addition of radiolabeled probe (30 min, 30°C) and separated by non-denaturing polyacrylamide gel electrophoresis and autoradiographic detection.

Cell Transfection and RNA Interference

MDAH2774 (2.5×10^6) and LN-17 (2.0×10^6) cells were transfected with siRNAs with the Amaxa Nucleofector (Amaxa) according to the manufacturer's protocol. MDAH2774 Cells were transfected with 100 nM siRNA using Amaxa Solution-L and program A-033. LN-17 cells were transfected with 300 nM (LN-17) siRNA using Amaxa Solution-R and program T-009. A GFP-expressing plasmid (Amaxa) was used to determine transfection efficiency. Silencer GAPDH siRNA, nonsilencing siRNA, silencer validated Jak1 (42841 and 219), Jak2 siRNAs (607 and 608), and Tyk2 siRNA (399 and 398) were purchased from Ambion. Cells were plated in a poly-L-Lycine coated 6 well plate (BD Biosciences) and incubated at 37°C/0.5% CO_2 for 24 and 48 hr. Cell lysates were collected for immunoblotting.

Tumor Models

Tumor studies were performed as previously described (Hedvat et al., 2004). Four to six week old athymic mice were purchased from Taconic Laboratories and acclimated for at least 3 days prior to tumor implantation. Mice bearing MDAH2774 xenografts were maintained under specific pathogen-free conditions and were used in compliance with protocols approved by the Institutional Animal Care and Use Committees of AstraZeneca, which conform to institutional and national regulatory standards on experimental animal usage. All remaining animal model studies were used in compliance with protocols approved by the Institutional Animal Care and Use Committees of City of Hope. Cell lines were subcutaneously implanted in athymic mice for MEF-Stat3-YFP, DU145, MDA-MB-468, and MDA-MB-468 cells expressing Stat3 shRNA or vector alone and 786-0 cells expressing pRC-vector or pRC-Stat3C in a 1:1 mixture of Matrigel (BD Biosciences) and culture medium. Cell lines were subcutaneously implanted in athymic mice with PBS for MDAH2774 cells. Tumor-bearing mice were randomized based on tumor volume prior to the initiation of treatment, which was initiated when average tumor volume was at least 65 mm^3. AZD1480 was given orally, as indicated in water supplemented with 0.5% Hypermellose and 0.1% Tween 80. Tumors were measured every 3 to 4 days with vernier calipers, and tumor volumes were calculated by the formula 0.5 × (larger diameter) × (smaller diameter)^2.

Statistical Analysis of Tumor Models

Tumor growth inhibition is calculated as 1 − T/C. T/C = (DT/DC) × 100, where T > 0, or %T/C = (DT/T1) × 100, where DT < 0. DT is the change of tumor volume in the treatment group, DC is that for the control group, and T1 is the mean tumor volume at the start of treatment.

p values indicated for animal efficacy studies consisting of two cohorts, LN-17 cell-line-derived data or CBC data, were derived with a Student's t test. Statistical analysis of the MDAH2774 xenograft study was performed with one-way ANOVA and p values were corrected for multiple comparisons to control by Dunnett's method.

SUPPLEMENTAL DATA

Supplemental Data include eight figures and can be found with this article online at http://www.cell.com/cancer-cell/supplemental/S1535-6108(09)00384-5.

ACKNOWLEDGMENTS

We thank Brenda Speer, Tony Cheung, Shelly Fang, Alan Rosen, Nancy Su, and Jiaquan Wu for technical assistance. D.H., J.M.G., A.S., D.P., G.B., S.W., L.W., M.Y., K.M., H.C., D.M., K.B., M.A., S.I., P.M., Z.A.C., and M.Z. are employees of AstraZeneca Pharmaceuticals. This work was supported in part by National Institutes of Health grant CA115674 and AstraZeneca.

Received: March 9, 2009
Revised: August 26, 2009
Accepted: October 16, 2009
Published: December 7, 2009

REFERENCES

Akira, S., Nishio, Y., Inoue, M., Wang, X.J., Wei, S., Matsusaka, T., Yoshida, K., Sudo, T., Naruto, M., and Kishimoto, T. (1994). Molecular cloning of APRF, a novel IFN-stimulated gene factor 3 p91-related transcription factor involved in the gp130-mediated signaling pathway. Cell *77*, 63–71.

Berishaj, M., Gao, S.P., Ahmed, S., Leslie, K., Al-Ahmadie, H., Gerald, W.L., Bornmann, W., and Bromberg, J.F. (2007). Stat3 is tyrosine-phosphorylated through the interleukin-6/glycoprotein 130/Janus kinase pathway in breast cancer. Breast Cancer Res. *9*, R32.

Boccaccio, C., Ando, M., Tamagnone, L., Bardelli, A., Michieli, P., Battistini, C., and Comoglio, P.M. (1998). Induction of epithelial tubules by growth factor HGF depends on the STAT pathway. Nature *391*, 285–288.

Bowman, T., Garcia, R., Turkson, J., and Jove, R. (2000). STATs in oncogenesis. Oncogene *19*, 2474–2488.

Bowman, T., Broome, M.A., Sinibaldi, D., Wharton, W., Pledger, W.J., Sedivy, J.M., Irby, R., Yeatman, T., Courtneidge, S.A., and Jove, R. (2001). Stat3-mediated Myc expression is required for Src transformation and PDGF-induced mitogenesis. Proc. Natl. Acad. Sci. USA *98*, 7319–7324.

Bromberg, J.F., Wrzeszczynska, M.H., Devgan, G., Zhao, Y., Pestell, R.G., Albanese, C., and Darnell, J.E., Jr. (1999). Stat3 as an oncogene. Cell *98*, 295–303.

Catlett-Falcone, R., Landowski, T.H., Oshiro, M.M., Turkson, J., Levitzki, A., Savino, R., Ciliberto, G., Moscinski, L., Fernandez-Luna, J.L., Nunez, G., et al. (1999). Constitutive activation of Stat3 signaling confers resistance to apoptosis in human U266 myeloma cells. Immunity *10*, 105–115.

Culig, Z., Steiner, H., Bartsch, G., and Hobisch, A. (2005). Interleukin-6 regulation of prostate cancer cell growth. J. Cell. Biochem. *95*, 497–505.

Darnell, J.E., Jr. (1997). STATs and gene regulation. Science *277*, 1630–1635.

Darnell, J.E., Jr., Kerr, I.M., and Stark, G.R. (1994). Jak-STAT pathways and transcriptional activation in response to IFNs and other extracellular signaling proteins. Science *264*, 1415–1421.

Dhir, R., Ni, Z., Lou, W., DeMiguel, F., Grandis, J.R., and Gao, A.C. (2002). Stat3 activation in prostatic carcinomas. Prostate *51*, 241–246.

Gao, S.P., Mark, K.G., Leslie, K., Pao, W., Motoi, N., Gerald, W.L., Travis, W.D., Bornmann, W., Veach, D., Clarkson, B., and Bromberg, J.F. (2007). Mutations in the EGFR kinase domain mediate STAT3 activation via IL-6 production in human lung adenocarcinomas. J. Clin. Invest. *117*, 3846–3856.

Garcia, R., Bowman, T.L., Niu, G., Yu, H., Minton, S., Muro-Cacho, C.A., Cox, C.E., Falcone, R., Fairclough, R., Parsons, S., et al. (2001). Constitutive activation of Stat3 by the Src and JAK tyrosine kinases participates in growth regulation of human breast carcinoma cells. Oncogene *20*, 2499–2513.

Gozgit, J.M., Bebernitz, G., Patil, P., Ye, M., Parmentier, J., Wu, J., Su, N., Wang, T., Ioannidis, S., Davies, A., et al. (2008). Effects of the JAK2 inhibitor, AZ960, on Pim/BAD/BCL-xL survival signaling in the human JAK2 V617F cell line SET-2. J. Biol. Chem. *283*, 32334–32343.

Grandis, J.R., Drenning, S.D., Zeng, Q., Watkins, S.C., Melhem, M.F., Endo, S., Johnson, D.E., Huang, L., He, Y., and Kim, J.D. (2000). Constitutive activation of Stat3 signaling abrogates apoptosis in squamous cell carcinogenesis in vivo. Proc. Natl. Acad. Sci. USA *97*, 4227–4232.

Grivennikov, S., and Karin, M. (2008). Autocrine IL-6 signaling: A key event in tumorigenesis? Cancer Cell *13*, 7–9.

Grivennikov, S., Karin, E., Terzic, J., Mucida, D., Yu, G.Y., Vallabhapurapu, S., Scheller, J., Rose-John, S., Cheroutre, H., Eckmann, L., and Karin, M. (2009). IL-6 and stat3 are required for survival of intestinal epithelial cells and development of colitis-associated cancer. Cancer Cell *15*, 103–113.

Guschin, D., Rogers, N., Briscoe, J., Witthuhn, B., Watling, D., Horn, F., Pellegrini, S., Yasukawa, K., Heinrich, P., Stark, G.R., et al. (1995). A major role for the protein tyrosine kinase JAK1 in the JAK/STAT signal transduction pathway in response to interleukin-6. EMBO J. *14*, 1421–1429.

Hedvat, M., Jain, A., Carson, D.A., Leoni, L.M., Huang, G., Holden, S., Lu, D., Corr, M., Fox, W., and Agus, D.B. (2004). Inhibition of HER-kinase activation prevents ERK-mediated degradation of PPARgamma. Cancer Cell *5*, 565–574.

Herrmann, A., Sommer, U., Pranada, A.L., Giese, B., Kuster, A., Haan, S., Becker, W., Heinrich, P.C., and Muller-Newen, G. (2004). STAT3 is enriched in nuclear bodies. J. Cell Sci. *117*, 339–349.

Hintzen, C., Evers, C., Lippok, B.E., Volkmer, R., Heinrich, P.C., Radtke, S., and Hermanns, H.M. (2008). Box 2 region of the Oncostatin M receptor determines specificity for recruitment of Janus kinases and STAT5 activation. J. Biol. Chem. *283*, 19465–19477.

Hodge, D.R., Hurt, E.M., and Farrar, W.L. (2005). The role of IL-6 and STAT3 in inflammation and cancer. Eur. J. Cancer *41*, 2502–2512.

Hong, D.S., Angelo, L.S., and Kurzrock, R. (2007). Interleukin-6 and its receptor in cancer: implications for Translational Therapeutics. Cancer *110*, 1911–1928.

Johnston, J.A., Kawamura, M., Kirken, R.A., Chen, Y.Q., Blake, T.B., Shibuya, K., Ortaldo, J.R., McVicar, D.W., and O'Shea, J.J. (1994). Phosphorylation and activation of the Jak-3 Janus kinase in response to interleukin-2. Nature *370*, 151–153.

Lacronique, V., Boureux, A., Monni, R., Dumon, S., Mauchauffe, M., Mayeux, P., Gouilleux, F., Berger, R., Gisselbrecht, S., Ghysdael, J., and Bernard, O.A. (2000). Transforming properties of chimeric TEL-JAK proteins in Ba/F3 cells. Blood *95*, 2076–2083.

Lam, L.T., Wright, G., Davis, R.E., Lenz, G., Farinha, P., Dang, L., Chan, J.W., Rosenwald, A., Gascoyne, R.D., and Staudt, L.M. (2008). Cooperative signaling through the signal transducer and activator of transcription 3 and nuclear factor-{kappa}B pathways in subtypes of diffuse large B-cell lymphoma. Blood *111*, 3701–3713.

Leaman, D.W., Leung, S., Li, X., and Stark, G.R. (1996). Regulation of STAT-dependent pathways by growth factors and cytokines. FASEB J. *10*, 1578–1588.

Lee, S.O., Lou, W., Hou, M., de Miguel, F., Gerber, L., and Gao, A.C. (2003). Interleukin-6 promotes androgen-independent growth in LNCaP human prostate cancer cells. Clin. Cancer Res. *9*, 370–376.

Levine, R.L., and Gilliland, D.G. (2008). Myeloproliferative disorders. Blood *112*, 2190–2198.

Levy, D.E., and Inghirami, G. (2006). STAT3: A multifaceted oncogene. Proc. Natl. Acad. Sci. USA *103*, 10151–10152.

Lo, H.W., Hsu, S.C., Xia, W., Cao, X., Shih, J.Y., Wei, Y., Abbruzzese, J.L., Hortobagyi, G.N., and Hung, M.C. (2007). Epidermal growth factor receptor cooperates with signal transducer and activator of transcription 3 to induce epithelial-mesenchymal transition in cancer cells via up-regulation of TWIST gene expression. Cancer Res. *67*, 9066–9076.

Lou, W., Ni, Z., Dyer, K., Tweardy, D.J., and Gao, A.C. (2000). Interleukin-6 induces prostate cancer cell growth accompanied by activation of stat3 signaling pathway. Prostate *42*, 239–242.

Manfredi, M.G., Ecsedy, J.A., Meetze, K.A., Balani, S.K., Burenkova, O., Chen, W., Galvin, K.M., Hoar, K.M., Huck, J.J., LeRoy, P.J., et al. (2007). Antitumor activity of MLN8054, an orally active small-molecule inhibitor of Aurora A kinase. Proc. Natl. Acad. Sci. USA *104*, 4106–4111.

Morgan, K.J., and Gilliland, D.G. (2008). A role for JAK2 mutations in myeloproliferative diseases. Annu. Rev. Med. *59*, 213–222.

Niu, G., Bowman, T., Huang, M., Shivers, S., Reintgen, D., Daud, A., Chang, A., Kraker, A., Jove, R., and Yu, H. (2002a). Roles of activated Src and Stat3 signaling in melanoma tumor cell growth. Oncogene *21*, 7001–7010.

Niu, G., Wright, K.L., Huang, M., Song, L., Haura, E., Turkson, J., Zhang, S., Wang, T., Sinibaldi, D., Coppola, D., et al. (2002b). Constitutive Stat3 activity up-regulates VEGF expression and tumor angiogenesis. Oncogene *21*, 2000–2008.

Okamoto, M., Lee, C., and Oyasu, R. (1997). Interleukin-6 as a paracrine and autocrine growth factor in human prostatic carcinoma cells in vitro. Cancer Res. *57*, 141–146.

Pranada, A.L., Metz, S., Herrmann, A., Heinrich, P.C., and Muller-Newen, G. (2004). Real time analysis of STAT3 nucleocytoplasmic shuttling. J. Biol. Chem. *279*, 15114–15123.

Quesnelle, K.M., Boehm, A.L., and Grandis, J.R. (2007). STAT-mediated EGFR signaling in cancer. J. Cell. Biochem. *102*, 311–319.

Rabinovich, A., Medina, L., Piura, B., Segal, S., and Huleihel, M. (2007). Regulation of ovarian carcinoma SKOV-3 cell proliferation and secretion of MMPs by autocrine IL-6. Anticancer Res. *27*, 267–272.

Schindler, C., and Darnell, J.E., Jr. (1995). Transcriptional responses to polypeptide ligands: the JAK-STAT pathway. Annu. Rev. Biochem. *64*, 621–651.

Silver, D.L., Naora, H., Liu, J., Cheng, W., and Montell, D.J. (2004). Activated signal transducer and activator of transcription (STAT) 3: localization in focal adhesions and function in ovarian cancer cell motility. Cancer Res. *64*, 3550–3558.

Wagner, B.J., Hayes, T.E., Hoban, C.J., and Cochran, B.H. (1990). The SIF binding element confers sis/PDGF inducibility onto the c-fos promoter. EMBO J. *9*, 4477–4484.

Wang, Y.Z., Wharton, W., Garcia, R., Kraker, A., Jove, R., and Pledger, W.J. (2000). Activation of Stat3 preassembled with platelet-derived growth factor beta receptors requires Src kinase activity. Oncogene *19*, 2075–2085.

Xi, S., Zhang, Q., Dyer, K.F., Lerner, E.C., Smithgall, T.E., Gooding, W.E., Kamens, J., and Grandis, J.R. (2003). Src kinases mediate STAT growth pathways in squamous cell carcinoma of the head and neck. J. Biol. Chem. *278*, 31574–31583.

Xin, H., Zhang, C., Herrmann, A., Du, Y., Figlin, R., and Yu, H. (2009). Sunitinib inhibition of Stat3 induces renal cell carcinoma tumor cell apoptosis and reduces immunosuppressive cells. Cancer Res. *69*, 2506–2513.

Yu, C.L., Meyer, D.J., Campbell, G.S., Larner, A.C., Carter-Su, C., Schwartz, J., and Jove, R. (1995). Enhanced DNA-binding activity of a Stat3-related protein in cells transformed by the Src oncoprotein. Science *269*, 81–83.

Yu, H., and Jove, R. (2004). The STATs of cancer—new molecular targets come of age. Nat. Rev. Cancer *4*, 97–105.

Yu, H., Kortylewski, M., and Pardoll, D. (2007). Crosstalk between cancer and immune cells: role of STAT3 in the tumour microenvironment. Nat. Rev. Immunol. *7*, 41–51.